

A Vanadium Alumanyl Complex: Synthesis, Characterization, Reactivity, and Application as a Catalyst for C–H Alumanylation of Alkenes

Pavel Zatsepin,^a Takumi Moriyama,^b Chaoqi Chen,^b Satoshi Muratsugu,^{b,c} Mizuki Tada,^{b,c,d} Makoto Yamashita^{*,a,c}

^a Department of Molecular and Macromolecular Chemistry, Graduate School of Engineering, Nagoya University, Furo-cho, Chikusa-ku, Nagoya, 464-8603 Aichi, Japan

^b Department of Chemistry, Graduate School of Science, Nagoya University, Furo-cho, Chikusa-ku, Nagoya, 464-8603 Aichi, Japan

^c Integrated Research Consortium on Chemical Science (IRCCS), Nagoya University, Tokai National Higher Education and Research System, Furo-cho, Chikusa-ku, Nagoya 464-8602, Japan

^d Research Center for Materials Science (RCMS), Nagoya University, Furo-cho, Chikusa-ku, Nagoya, 464-8602 Aichi, Japan

ABSTRACT: A complex containing a V–Al bond is described. This species can be prepared by either transmetallation of a previously disclosed alumanylpotassium with Cp₂VCl or photolytic oxidative alumination of Cp₂V using the corresponding dialumane(4). Reaction of the resulting V–Al complex with H₂ gave a Cp₂V–dihydridoaluminate complex. These complexes were studied with X-ray crystallography, spectroscopy including vanadium *K*-edge XANES spectroscopy, and DFT calculations. Finally, the reactivity of these molecules was studied opening the way to a catalytic C–H alumanylation of alkenes.

Complexes featuring an X-type alumanyl ligand coordinated to a transition metal (TM) centre are quite rare. Although the first example was published over 25 years ago (Figure 1, **A**),¹ this subject had remained relatively dormant until the recent advent of alkali metal salts of alumanyl anions² as precursors in transmetallation reactions with TM halides (Figure 1, **B, C**).³ Since aluminum has a low electronegativity (1.61, Pauling scale),⁴ leading to a strong σ -donating character as a ligand, these complexes exhibited nucleophilic reactivity at the metal center.³ However, despite recent advances, reports of TM–alumanyls have still generally been limited to late TMs with only three group 3 TM–Al complexes (Figure 1, **D, E**) standing as exceptions.⁵ Given that the electronegativities of group 4 and 5 TMs are similar to that of Al, group 4 and 5 TM–Al bonds would represent a polarity-covalency regime that has yet to be surveyed. Herein, we report a V–Al complex with its synthesis, characterisation, reactivity, and application as a catalyst for C–H alumanylation of alkenes.

A salt elimination reaction between our previously reported diamino-Al anion **1** with one equivalent of Cp₂VCl afforded a V–Al complex **2** in 82% yield (Scheme 1). This complex **2** can also be generated by irradiation of the mixture consisting of Cp₂V and dialumane **3** with UV-B light at a sluggish pace. It should be noted that the synthesis of gallyl-vanadocene species (Figure 1, **F**)⁶ using digallane in the presence of Cp₂V was reported without irradiation of UV-B light. Although **2** exhibited only broad resonances in ¹H NMR spectroscopy due to its paramagnetic character, single-crystal X-ray diffraction (sc-XRD) revealed the structure of **2**. The V–Al distance of 2.5999(6) Å was shorter than the sum of the covalent radii (2.74 Å). Angles about the Al centre sum to 359.55°, indicating a

trigonal-planar geometry about the Al atom. A magnetic moment of 2.70 μ_B was observed by SQUID between 55K and 400K, somewhat under the spin-only value for an *S* = 1 spin system, 2.83 μ_B . Due to high spin V(III) being a non-Kramers ion, **2** is EPR-silent in X- and Q-band experiments; the zero field splitting is likely too great for a transition to be observed in the field-frequency window available to the instruments used. The UV-Vis spectrum of **2** (Figure S4) shows two peaks at 705 nm (127 M⁻¹ cm⁻¹) and 590 nm (236 M⁻¹ cm⁻¹), assignable to the *d*–*d* transitions from the V-centred highest- and second highest-energy SOMOs to vacant orbitals of metal-ligand antibonding character, that are expected in this bent metallocene complex.⁷

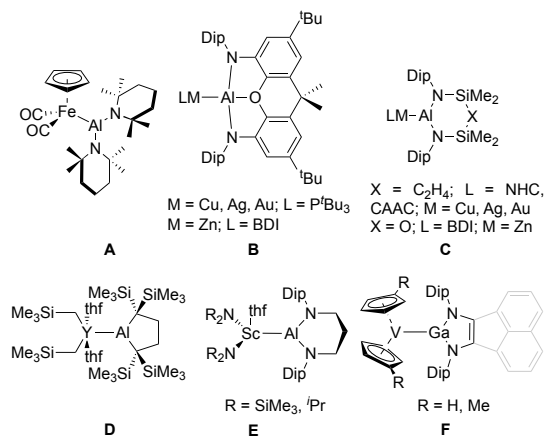
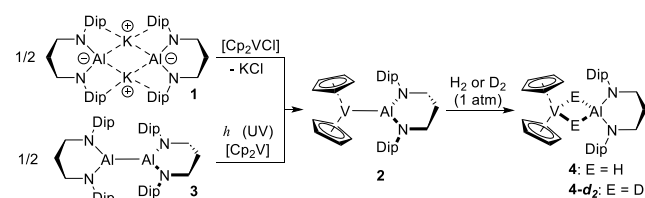


Figure 1. Previous examples of transition metal alumanyl complexes. Dip = 2,6-diisopropylphenyl.

Scheme 1. Synthesis of V–Al complex **2** and its reaction with H₂ or D₂.



Under an atmosphere of hydrogen gas, **2** was converted to **4** possessing two bridging hydride ligands with a color change from blue-green to pale red. The resulting **4** is diamagnetic and provides a sharp set of signals in its ¹H NMR spectrum. A singlet at 3.92 ppm

corresponds to the Cp ligands while another singlet at -13.72 ppm is consistent with the presence of two hydride ligands, and the remaining resonances can be assigned to the diamino ligand. Although no ^{27}Al NMR signal of **4** was observed, a broad signal was found at -1105 ppm ($\nu_{1/2} = 1300$ Hz) in the ^{51}V NMR spectrum. The IR spectrum of **4** exhibited a strong absorption at 1535 cm^{-1} , that can be assigned as M–H vibration. Disappearance of this absorption in the IR spectrum of **4-d₂** (Fig. S14), similarly prepared from **2** with D_2 , confirms the assignment, that is also supported by the vibrational analysis using DFT calculations (1612 and 1640 cm^{-1} , unscaled, see Fig. S63). The sc-XRD using crystals of **4** revealed a V–Al distance of $2.530(1)\text{ \AA}$, notably shorter than that found in **2**. The bridging hydrides could be located from the differential Fourier map, and the angle between the H–Al–H and N–Al–N planes is 31.08° off from the idealized, 90° orientation. This distortion is likely a consequence of steric restrictions imposed by clashing of the diamino ligand and Cp ligands.

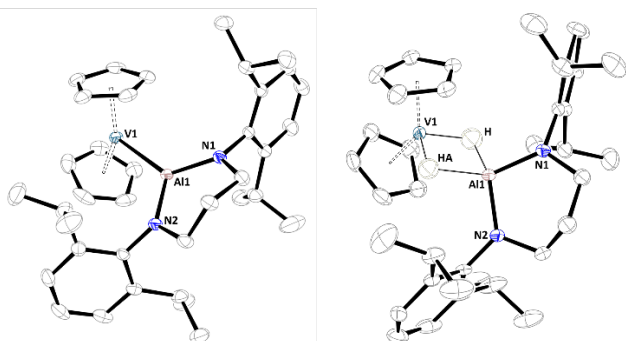


Figure 2. Crystal structures of **2** (left) and **4** (right) with thermal ellipsoids at the 50% probability level. H-atoms except hydride ligands (**4**) and co-crystallized solvent (**4**) omitted for clarity.

Although the above data clarifies the connectivity of **2** and **4**, the electronic structure is somewhat ambiguous because both Al and V atoms have similar electronegativity (Al: 1.61, V: 1.63, Pauling)⁴ and flexibility in their oxidation states.⁸ Polarization of the V–Al bond in **2** would have two possibilities as described in Figure 3(a). In case it is polarized as $\text{V}^+ \cdots \text{Al}^-$, **2** can be considered as alumanyl [Al(I)]–V(III) complex **2-I** with retention of Al-anion character – similar to that of the previously reported Al–Sc complex.^{5b} If it would be polarized as $\text{V}^- \cdots \text{Al}^+$, **2** should be considered as vanadocenyl(I) anion-substituted diaminoaluminum **2-II**, formed *via* two-electron reduction of the V(III) center by Al(I) reagent. Considering the similar polarization between V and Al atoms and the related group 5 metallocene hydridoborate species,⁹ one can speculate that **4** has three possible bonding situations [Figure 3(b)]. If V and Al atoms still have a polarized bond as $\text{V}^+ \cdots \text{Al}^-$, **4** should be described as alumanyl [Al(I)]–V(V)H₂ complex **4-I**, that would be consistent with the shorter V–Al distance in **4** than in **2**. The opposite polarization having $\text{V}^- \cdots \text{Al}^+$ character would provide dihydrovanadate(III) anion-coordinated diaminoaluminum **4-II**. In case two hydrogen atoms attached to the Al atom, it should be considered as $(\text{N}_2\text{AlH}_2)^-$ anion-coordinated cationic vanadocene **4-III** through μ^2 -H₂Al coordination mode or two V–H–Al 3c-2e bonds with the bridging hydrides. To gain experimental insight into the oxidation state, vanadium *K*-edge X-ray absorption near edge structure (XANES) spectroscopy was employed (Figure 4; See Fig S56. for more details). The edge energy of **2** was slightly lower than other V(III) compounds such as [Cp₂VCl] but notably higher than V(II) species such as [Cp₂V]. This may speak to the polar-covalent character of the V–Al bond with

significant sharing of electrons leading to a slightly reduced V(III) center. In contrast, the edge energy of **4** was found to be consistent with a V(III) oxidation state and clearly lower than those of V(IV) and V(V) species – strong evidence that assignment as **4-I** in the oxidation state of V(V) is not appropriate.

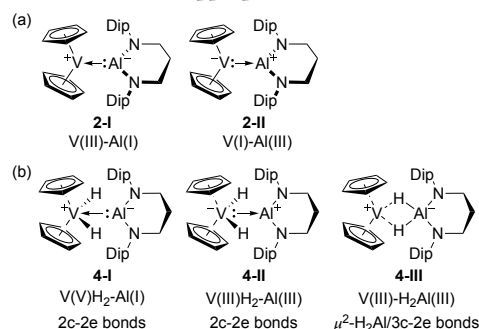


Figure 3. Several conceivable ways to describe bonding situation and oxidation state in **2** and **4**.

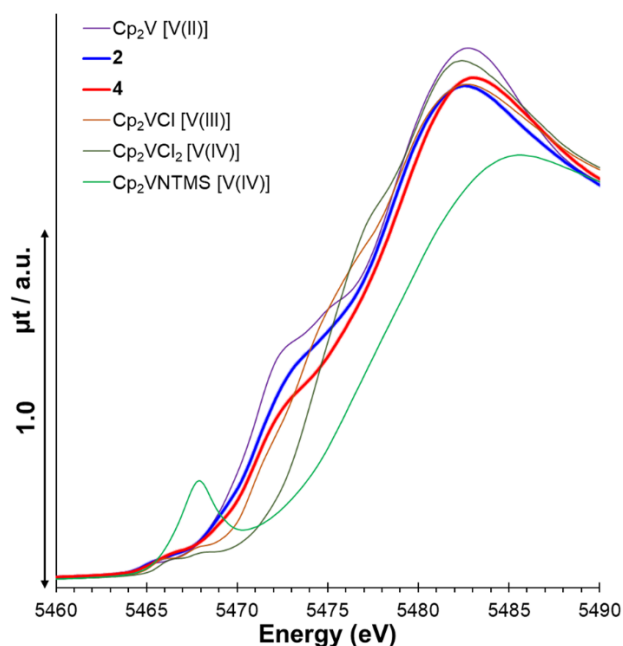


Figure 4. Vanadium *K*-edge XANES spectra of various reference compounds of vanadium in oxidation states (II) through (IV) and complexes **2** and **4**.

Further insight into the electronic structure and bonding of **2** and **4** was obtained with DFT calculations (see SI for further details). Computed geometries excellently reproduced those obtained by sc-XRD with the calculated V–Al distances of 2.6037 \AA (for **2**) and 2.512 \AA (for **4**). Quantum Theory of Atoms in Molecules (QTAIM) analysis was also performed (Figure 5). A bond critical point (BCP) was located along a path between V and Al atoms in **2** [Figure 5(a)] indicating the existence of a bonding interaction. The value of the Laplacian of electron density [$\nabla^2\rho$] at this BCP is -0.0612 and suggests that the V–Al bond in **2** is covalent, unlike species **E** in which the Sc–Al interaction was found to be ionic.⁵ The AIM basin charges (q) of V and Al were 0.888 and 1.786 respectively, hence $\Delta q_{\text{Al-V}} = 0.898$, a smaller charge difference than those calculated for covalently bonded Cu–, Ag–, Au–, or Zn–Al complexes is indicative of the less polarized V–Al bond in **2** relative to the late-TM–Al bonds.³ In the case of **4**, no BCP was found between the V and Al atoms; rather, there are curved bond paths and BCPs between each metal and the bridging hydrides with a ring critical point (RCP) in the

centre of the plane containing these four atoms [Figure 5(b)]. This result clearly indicates the existence of two 3c–2e bonds in V–H–Al moieties. Hence, forms **2-I** and **4-III** are consistent with the results obtained from XANES spectra and DFT calculations.

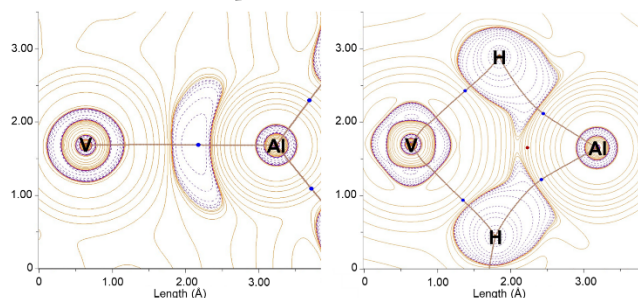
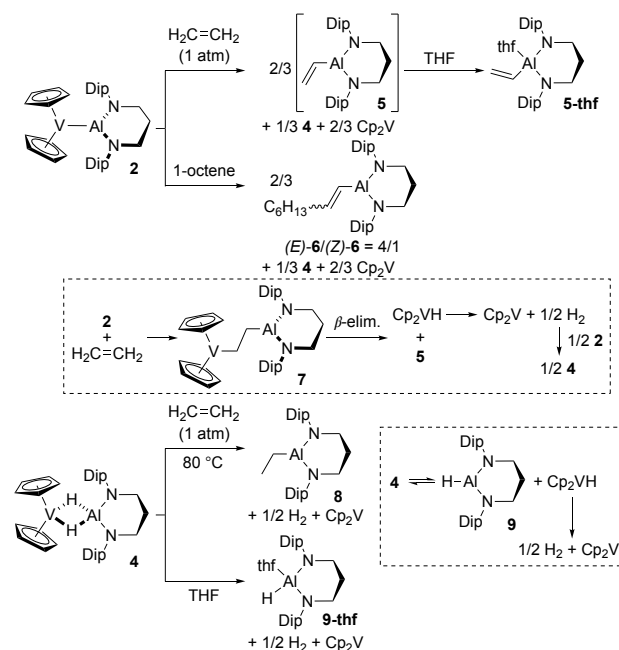


Figure 5. Topological QTAIM-derived plots of $\nabla^2\rho$ for **2** (left) and **4** (right). Solid, orange contours where $\nabla^2\rho > 0$; dashed, violet contours where $\nabla^2\rho < 0$. Blue dots are BCPs, crimson dots are RCPs, brown lines are bond paths.

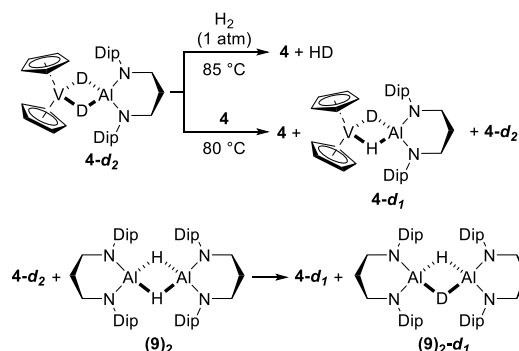
Reactivity of the V–Al bonded species **2** and its H₂ adduct **4** was also evaluated (Scheme 2). A C₆D₆ solution of **2** was exposed to 1 atm of ethylene at ambient temperature leading to a color change from blue-green to purple. The ¹H NMR spectrum of the final product mixture displayed a complete consumption of **2** and formation of **4** and vinylalumane **5** in a 1:2 ratio. The existence of **5** was strongly supported by vinylic NMR signals at 5.92 and 5.64 ppm (by comparison with those of independently prepared **5**, Fig. S15). Recrystallization of the residue of this sample from hexane with the addition of several drops of THF provided colourless single crystals of **5-thf** as identified by sc-XRD (Fig. S57). Similarly, a stoichiometric reaction between 1-octene and **2** gave 1-octenylalumanes (*E*)-**6**/*Z*)-**6** as a mixture in a 4/1 ratio with **4**. The identity of (*E*)-**6**/*Z*)-**6** was further confirmed by comparison to an independently prepared sample as well by subsequent iodination to liberate 1-octenyl iodide (Figs. S21, S55) The regiochemistry of (*E*)- and (*Z*)-isomer was assigned with a characteristic ³J_{HH} coupling constant. We propose that this aluminium reaction proceeds through a 1,2-insertion of alkenes to V–Al bond to afford 1,2-dimetallated alkane **7**, a step that was recently demonstrated by Crimmin for Fe–Al bonds,¹⁰ followed by a β-hydride elimination with putative formation of [Cp₂VH], which could decompose to Cp₂V with spontaneous generation of H₂.¹¹ In fact, we observed a purple color confirmed as Cp₂V by UV-Vis (Figure S39) after the reaction finished. Although **4** did not react with atmospheric ethylene at ambient temperature, heating at 80 °C led to the formation of an ethylalumane **8** with consumption of **4**. Since this represents a hydroalumination of ethylene, we assumed the dissociation of hydroalumane intermediate **9** from **4**. In fact, dissolution of **4** in THF-*d*₈ leads to noticeable colour change from red to purple with visible effervescence of H₂ and **9-thf-d8** was identified in the ¹H NMR spectrum.

Scheme 2. Reactions of **2** and **4** with alkenes and THF.



To confirm the dissociation of **8** from **4**, an isotopic labeling experiment was performed with deuterium-enriched **4-d₂** (Scheme 3). Heating **4-d₂** under 1 atm of H₂ in C₆D₆ at 85 °C led to a gradual increase of the characteristic hydride signal of **4** at –13.72ppm with an appearance of a triplet signal of HD in the ¹H NMR spectrum. We hypothesise that the formation of HD may be mediated by [Cp₂VD] which should be generated from **4-d₂** as this kind of reaction is known for [Cp₂MH] (M = Nd, Ta) and [Cp₂*VH] complexes.¹² Following the 1:1 mixture of **4-d₂** and **4** and heating at 80 °C, ¹H NMR spectroscopy at –50 °C displayed two sets of hydride signals indicative of the presence of **4-d₁** alongside **4**. Finally, addition of independently synthesized (**9**)₂ to **4-d₂** resulted in the appearance of a hydride signal of **4-d₁** at –13.69 ppm further supporting the lability of **9** and the putative [Cp₂VH] from **4**.

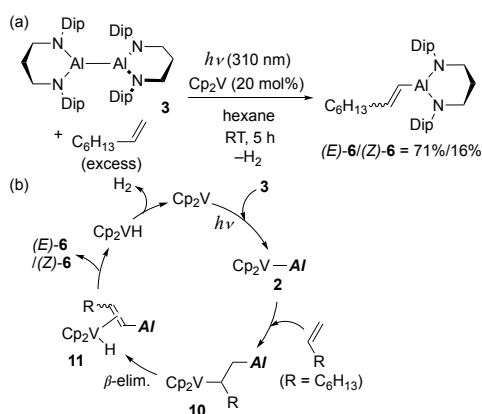
Scheme 3. Isotope labelling experiments probing the equilibrium between **4** and **9**+Cp₂VH.



Considering all the reactions described here, we noticed the potential for Cp₂V to act as a catalyst in the C–H aluminylation of alkenes in the presence of dialumane **3** under irradiation of UV-B light. Mixing **3** with a large excess of 1-octene and a catalytic amount of Cp₂V (10 mol% V to Al) in hexane under 310 nm irradiation at room temperature for 5 hours gave the corresponding 1-octenylalumanes (*E*)-**6**/*Z*)-**6** in 71%/16% yield as judged by the ¹H NMR spectrum of the crude mixture [Scheme 4(a)]. This is an unusual C–H functionalization in the context of vanadium chemistry; oxovanadium

compounds are well-known in C–H hydroxylation through a hydrogen abstraction mechanism.¹³ The catalytic cycle [Scheme 4(b)] would involve a photochemical generation of **2** from Cp₂V and **3**, insertion of 1-octene to form dimetallated alkane **10**, β-hydride elimination to afford **11**, dissociation of (*E*)-**6**/*Z*)-**6** to liberate Cp₂VH, and spontaneous H₂ evolution to regenerate Cp₂V, as the most of the elementary steps were experimentally confirmed. Considering the analogous vinylic C–H borylation reactions catalyzed by *late* TMs¹⁴ are widely used for organic transformation, the unprecedented C–H alumanylation in this work would also have an impact to the organic synthesis field.

Scheme 4. Photocatalytic dehydrogenative alumination of 1-octene by vanadocene catalyst.



In summary, the first instance of a complex containing a V–Al bond has been prepared by either salt metathesis or by a photochemical route. This V–Al complex **2** reacts with H₂ to yield a vanadium dihydridoaluminate **4**. Combination of XANES analysis and DFT calculations provided insights into the oxidation states of each metal atom and bonding situations in **2** with 2c–2e V–Al bond and **4** with 3c–2e V–H–Al bonds. The bridging hydride species **4** was also shown to be labile towards release of dihydridoalumane **9** and Cp₂VH as confirmed by control experiments. The vanadium alumanyl is also involved as an intermediate in a photocatalytic C–H alumanylation of alkenes using Cp₂V as a catalyst.

ASSOCIATED CONTENT

The Supporting Information is available free of charge on the ACS Publications website.

Experimental and computational details (PDF)

Crystallographic data for **1**, **2**, **5-thf**, **8**, and (**9**)₂ (CIF)

DFT coordinates (XYZ)

AUTHOR INFORMATION

Corresponding Author

* makoto@oec.chembio.nagoya-u.ac.jp

Notes

The authors declare no competing financial interest.

ACKNOWLEDGMENT

This research was supported by a Grant-in-Aid for Scientific Research (B) (JSPS KAKENHI grant 21H01915 for M.Y.) and Grant-in-Aid for Challenging Research (Exploratory) (JSPS KAKENHI grant 21K18978 for S.M.). P.Z. is grateful for a JSPS postdoctoral fellowship for research in Japan (PE21029). XAFS measurements were performed with the approval of PF-PAC (Nos. 2021G110, and 2021G113) and the Aichi

Synchrotron Radiation Center (No. 202206048). A part of the computation was performed using Research Center for Computational Science, Okazaki, Japan (Project: 22-IMS-C006, 23-IMS-C006). The authors thank to Profs. Kunio Awaga and Michio M. Matsushita (Nagoya University) for providing access to the SQUID instrument.

REFERENCES

- Anand, B. N.; Krossing, I.; Nöth, H. Synthesis and X-ray Crystal Structure of (tmp)₂Al–Fe(cp)(CO)₂: An Alanyl-Containing Iron Complex with a Tricoordinated Aluminum Atom. *Inorg. Chem.* **1997**, *36*, 1979–1981.
- a) Hicks, J.; Vasko, P.; Goicoechea, J. M.; Aldridge, S. The Aluminyl Anion: A New Generation of Aluminium Nucleophile. *Angew. Chem. Int. Ed.* **2021**, *60*, 1702–1713. b) Coles, M. P.; Evans, M. J. The emerging chemistry of the aluminyl anion. *Chem. Commun.* **2023**, *59*, 503–519.
- a) Hicks, J.; Mansikkamäki, A.; Vasko, P.; Goicoechea, J. M.; Aldridge, S. A nucleophilic gold complex. *Nat. Chem.* **2019**, *11*, 237–241. b) McManus, C.; Hicks, J.; Cui, X.; Zhao, L.; Frenking, G.; Goicoechea, J. M.; Aldridge, S. Coinage metal aluminyl complexes: probing regiochemistry and mechanism in the insertion and reduction of carbon dioxide. *Chem. Sci.* **2021**, *12*, 13458–13468. c) Liu, H.-Y.; Neale, S. E.; Hill, M. S.; Mahon, M. F.; McMullin, C. L. On the reactivity of Al-group 11 (Cu, Ag, Au) Bonds. *Dalton Trans.* **2022**, *51*, 3913–3924. d) Evans, M. J.; Iliffe, G. H.; Neale, S. E.; McMullin, C. L.; Fulton, J. R.; Anker, M. D.; Coles, M. P. Isolating elusive ‘Al(μ-O)’ intermediates in CO₂ reduction by bimetallic Al–M complexes (M = Zn, Mg). *Chem. Commun.*, **2022**, *58*, 10091–10094.
- Pauling, L. Chapter 3: The Partial Ionic Character of Covalent Bonds and the Relative Electronegativity of Atoms. *Nature of the Chemical Bond*, 3rd ed.; Cornell University Press: Ithaca, NY, 1960; p 93.
- a) Sugita, K.; Yamashita, M. An Alumanyltrium Complex with an Absorption due to a Transition from the Al–Y Bond to an Unoccupied d-Orbital. *Chem. Eur. J.* **2020**, *26*, 4520–4523. b) Feng, G.; Chan, K. L.; Lin, Z.; Yamashita, M. Al–Sc Bonded Complexes: Synthesis, Structure, and Reaction with Benzene in the Presence of Alkyl Halide. *J. Am. Chem. Soc.* **2022**, *144*, 22662–22668.
- a) Aldridge, S.; Baker, R. J.; Coombs, N. D.; Jones, C.; Rose, R. P.; Rossin, A.; Willock, D. J. Complexes of a gallium heterocycle with transition metal dicyclopentadienyl and cyclopentadienylcarbonyl fragments, and with a dialkylmanganese compound. *Dalton Trans.* **2006**, 3313–3320. b) Fedushkin, I. L.; Sokolov, V. G.; Makarov, V. M.; Cherkasov, A. V.; Abakumov, G. A. Transition metal 1,3,2-diazagallol derivatives. *Russ. Chem. Bull.* **2016**, *65*, 1495–1504.
- a) Green, J. C.; Payne, M. P.; Teuben, J. H. He I and He II Photoelectron Studies of Bis(cyclopentadienyl)vanadium(III) Complexes. *Organometallics*, **1983**, *2*, 203–210. b) Lukens, W. W.; Smith, M. R. III.; Andersen, R. A. A π-Donor Spectrochemical Series for X in (Me₅C₅)₂TiX, and β-Agostic Interactions in X = Et and N(Me)Ph. *J. Am. Chem. Soc.* **1996**, *118*, 1719–1728.
- The following papers discussed about oxidation state of the Al center by using XANES or XPS spectra. a) Altman, A. B.; Pemmaraju, C. D.; Camp, C.; Arnold, J.; Minasian, S. G.; Prendergast, D.; Shuh, D. K.; Tylliszczak, T. Theory and X-ray Absorption Spectroscopy for Aluminum Coordination Complexes – Al K-Edge Studies of Charge and Bonding in (BDI)Al, (BDI)AlR₂, and (BDI)AlX₂ Complexes. *J. Am. Chem. Soc.* **2015**, *137*, 10304–10316. b) Hooper, T. N.; Lau, S.; Chen, W.; Brown, R. K.; Garçon, M.; Luong, K.; Barrow, N. S.; Tatton, A. S.; Sackman, G. A.; Richardson, C.; White, A. J. P.; Cooper, R. I.; Edwards, A. J.; Casely, I. J.; Crimmin, M. R. The partial dehydrogenation of aluminium dihydrides. *Chem. Sci.* **2019**, *10*, 8083–8093. c) Kurumada, S.; Yamanashi, R.; Sugita, K.; Ito, H.; Ikemoto, S.; Chen, C.; Moriyama, T.; Muratsugu, S.; Tada, M.; Koitaya, T.; Ozaki, T.; Yamashita, M. Mechanochemical Synthesis of Non-Solvated Dialkylaluminyl Anion and XPS Characterization of Al(I) and Al(II) Species. *ChemRxiv*. DOI: 10.26434/chemrxiv-2023-9h7z1-v2
- a) Hartwig, J. F.; De Gala, S. R. A Continuum Resulting from Equilibrium between Two Structural Extremes in Tungstenocene and Niobocene Boryl and Hydridoborate Complexes. π-Bonding in a d³ Boryl System and the First d⁰ Boryl Complex. *J. Am. Chem. Soc.* **1994**, *116*, 3661–3662. b) Lantero, D. R.; Motry, D. H.; Ward, D. L.; Smith, M. R. III. Synthesis of endo-

$\text{Cp}_2\text{TaH}_2(\text{BO}_2\text{C}_6\text{H}_4)$ and $\text{exo-Cp}_2\text{TaH}_2(\text{BO}_2\text{C}_6\text{H}_4)$: Regioisomers of the First Tantalum Boryl Complexes. *J. Am. Chem. Soc.* **1994**, *116*, 10811–10812. c) Miyada, T.; Kwan, E. H.; Yamashita, M. Synthesis, Structure, and Bonding Properties of Ruthenium Complexes Possessing a Boron-Based PBP Pincer Ligand and Their Application for Catalytic Hydrogenation. *Organometallics* **2014**, *33*, 6760–6770. d) Morisako, S.; Watanabe, S.; Ikemoto, S.; Muratsugu, S.; Tada, M.; Yamashita, M. Synthesis of A Pincer-Ir^V Complex with A Base-Free Alumanyl Ligand and Its Application toward the Dehydrogenation of Alkanes. *Angew. Chem. Int. Ed.* **2019**, *58*, 15031–15035.

10. Gorgas, N.; Stadler, B.; White, A.; Crimmin, M. Vinylic C–H Activation of Styrenes by an Iron–Aluminum Complex. *ChemRxiv*, **2023**, DOI: 10.26434/chemrxiv-2023-57hwb.

11. a) Bouman, H. Teuben, J. H. Synthesis and properties of alkyldicyclopentadienylvanadium(III) compounds. *J. Organomet. Chem.* **1976**, *110*, 327–330. b) Mar'in, V. P.; Vyshinskaya, L. I.; Razuvaev, G. A. Thermal decomposition and photodecomposition of biscyclopentadienyl complexes of titanium, vanadium, and their analogues. *Russ. Chem. Rev.* **1989**, *58*, 494–506. c) Doerrer, L. H.; Green, M. L. H. Oxidation of $[\text{M}(\eta\text{-C}_5\text{H}_5)_2]$, M = Cr, Fe or Co, by the new Brønsted acid $\text{H}_2\text{O}\cdot\text{B}(\text{C}_6\text{F}_5)_3$ yielding the salts $[\text{M}(\eta\text{-C}_5\text{H}_5)_2]^+\text{A}^-$, where $\text{A}^- = [(\text{C}_6\text{F}_5)_3\text{B}(\mu\text{-OH})\text{B}(\text{C}_6\text{F}_5)_3]^-$ or $[(\text{C}_6\text{F}_5)_3\text{BOH} \cdots \text{H}_2\text{OB}(\text{C}_6\text{F}_5)_3]^-$. *J. Chem. Soc., Dalton Trans.* **1999**, 4325–4329.

12. a) Barfield, E. K.; Parshall, G. W.; Tebbe, F. N. Catalysis of aromatic hydrogen-deuterium exchange by metal hydrides. *J. Am. Chem. Soc.* **1970**, *92*, 5234–5235. b) Tebbe, F. N. Lewis acidic metal alkyl-transition metal complex interactions. I. Niobium and tantalum hydrides. *J. Am. Chem. Soc.* **1973**, *95*, 5412–5414. c) Curtis, C. J.; Smart, J. C.; Robbins, J. L. Synthesis of Methyl and Hydride Derivatives of Permethylvanadocene and their Reactions with Carbon Monoxide. *Organometallics*, **1985**, *4*, 1283–1286.

13. Langeslay, R. R.; Kaphan, D. M.; Marshall, C. L.; Stair, P. C.; Sattelberger, A. P.; Delferro, M. Catalytic Applications of Vanadium: A Mechanistic Perspective. *Chem. Rev.* **2019**, *119*, 2128–2191.

14. Mkhaldid, I. A. I.; Barnard, J. H.; Marder, T. B.; Murphy, J. M.; Hartwig, J. F. C–H Activation for the Construction of C–B Bonds. *Chem. Rev.* **2010**, *110*, 890–931.

